Rhodobacter capsulatus Contains a Novel *cb*-Type Cytochrome *c* Oxidase without a Cu_A Center†

Kevin A. Gray,‡ Michael Grooms,‡ Hannu Myllykallio,‡ Carolyn Moomaw,§ Clive Slaughter,§ and Fevzi Daldal*,‡

Plant Science Institute, Department of Biology, The University of Pennsylvania, Philadelphia, Pennsylvania 19104-6018, and Howard Hughes Medical Institute, University of Texas Southwest Medical Center at Dallas, Dallas, Texas 75235

Received November 22, 1993; Revised Manuscript Received January 18, 1994®

ABSTRACT: The facultative phototrophic bacterium *Rhodobacter capsulatus* is capable of growth in a wide range of environmental conditions using a highly branched electron-transfer chain. During respiratory growth of this organism reducing equivalents are conveyed to oxygen via two terminal oxidases, previously called "cyt b_{410}" (cytochrome *c* oxidase) and "cyt b_{260}" (quinol oxidase). The cytochrome *c* oxidase was purified to homogeneity from a semiaerobically grown *R. capsulatus* strain. The purified enzyme consumes oxygen at a rate of 600 s^{-1}, oxidizes reduced equine cyt *c* and *R. capsulatus* cyt c_2, and has high sensitivity to cyanide. The complex is composed of three major polypeptides of apparent molecular masses 45, 32, and 28 kDa on SDS–PAGE. The 32- and 28-kDa proteins also stain with tetramethylbenzidine, indicating that they are *c*-type cytochromes. Partial amino acid sequences obtained from each of the subunits reveal significant homology to the *fix*N, *fix*O, and *fix*P gene products of *Bradyrhizobium japonicum* and *Rhizobium meliloti*. The reduced enzyme has an optical absorption spectrum with distinct features near 550 and 560 nm and an asymmetric Soret band centered at 418 nm, indicating the presence of both *c*- and *b*-type cytochromes. Two electrochemically distinct cyt *c* are apparent, with redox midpoint potentials (E_{m7}) of 265 and 320 mV, while the low-spin cyt *b* has an E_{m7} value of 385 mV. The enzyme binds carbon monoxide, and the CO difference spectrum indicates that CO binds to a high-spin cyt *b*. Pyridine hemochrome and HPLC analyses suggest that the complex contains 1 mol of heme C to 1 mol of protoheme and that neither heme O nor heme A is present. Further, the *R. capsulatus* mutant M7 and its derivatives known to lack "cyt b_{410}" also lack the 32-kDa cyt *c* subunit, and redox titrations of the mutant membranes indicate that the 320-mV cyt *c* correlates with the remaining 28-kDa cyt *c*. Electron paramagnetic resonance spectroscopy of the purified enzyme performed at 10 and 77 K shows the presence of both low-spin and high-spin ferricytochromes, but in contrast to all other previously characterized cyt *c* oxidases, no indication for a Cu_A-like signal was found at either temperature. The overall data therefore indicate that *R. capsulatus* contains a novel *cb*-type cyt *c* oxidase without a Cu_A center.

The Gram-negative faculative photosynthetic bacterium, *Rhodobacter capsulatus*, can grow under a wide variety of conditions resulting in a highly branched energy-transducing electron transfer chain (Ferguson et al., 1987). Under phototrophic growth conditions the photosynthetic reaction center and the ubihydroquinone–cytochrome *c* oxidoreductase (cyt bc_1 complex)[1] participate in light-driven cyclic electron transfer, ultimately transporting protons across the intracytoplasmic membrane (Dutton, 1986; Cramer & Knaff, 1990). The proton electrochemical gradient is subsequently used for energy-requiring processes in the cell such as ATP synthesis, active transport, and taxis.

The proton-translocating respiratory electron transfer chain in *R. capsulatus* is branched after the quinone pool and involves two different terminal oxidases, previously called "cyt b_{410}" (cyt *c* oxidase, C_{ox}) and "cyt b_{260}" (quinol oxidase, Q_{ox}) (Marrs & Gest, 1973; Baccarini-Melandri et al., 1973; Zannoni et al., 1976; LaMonica & Marrs, 1976). One of these branches is quite similar to mitochondrial electron transfer in that it involves the cyt bc_1 complex and a cyt *c*. The final step of this branch is the four-electron reduction of molecular oxygen to water catalyzed by a cyt *c* oxidase. The second branch terminates with a quinol oxidase circumventing cyt *c* and the cyt bc_1 complex, and deriving electrons used to reduce O_2 to H_2O directly from the quinol pool (Zannoni et al., 1976; Baccarini-Melandri & Zannoni, 1978). Under dark, anaerobic conditions other compounds such as dimethyl sulfoxide (Yen & Marrs, 1977; Zannoni & Marrs, 1981), trimethylamine oxide, and nitrous oxide (McEwan et al., 1985) can serve as terminal electron acceptors. This metabolic versatility makes the purple non-sulfur bacteria useful organisms for the study of electron transfer pathways which may contain several as yet incompletely characterized redox-active proteins (Zannoni & Daldal, 1993).

Marrs and Gest (1973) isolated several *R. capsulatus* mutants which are defective in the respiratory electron transfer chain while still being proficient in photosynthesis. One such mutant, referred to as M5, is unable to catalyze the α-naphthol + dimethyl-*p*-phenylenediamine + O_2 → indophenol blue + H_2O reaction (NADI) and is deficient in the terminal oxidases (Marrs & Gest, 1973). Also isolated were two different spontaneous revertants of M5, called M6 and M7, which gained the ability to grow by respiration (Marrs & Gest, 1973).

† This work is supported by grants from NIH (GM 38237) and DOE (91ER20052).

* To whom correspondence should be addressed. Phone: 215-898-4394; FAX: 215-898-8780; Email: fdaldal@mail.sas.upenn.edu.

‡ The University of Pennsylvania.

§ University of Texas Southwest Medical Center at Dallas.

® Abstract published in *Advance ACS Abstracts,* February 15, 1994.

[1] Abbreviations: cyt, cytochrome; SDS–PAGE, sodium dodecyl sulfate–polyacrylamide gel electrophoresis; TMPD, *N,N,N′,N′*-tetramethyl-*p*-phenylenediamine; TMBZ, 3,3′,5,5′-tetramethylbenzidine; PMS, *N*-methyldibenzopyrazine methosulfate; E_{m7}, redox midpoint potential at pH 7; EPR, electron paramagnetic resonance; HPLC, high-pressure liquid chromatography.

0006-2960/94/0433-3120$04.50/0

M6 regained cyt *c* oxidase activity (remaining Q_{ox}^-), is $NADI^+$, and is sensitive to low concentrations of cyanide, while M7 regained quinol oxidase activity (remaining C_{ox}^-), is $NADI^-$, and is sensitive to CO. Biochemical analyses of these mutants led to the identification of the two terminal oxidases in *R. capsulatus* referred to as cyt b_{410} (cyt *c* oxidase) and cyt b_{260} (quinol oxidase), based upon the equilibrium redox midpoint potentials of their cyt *b* components (LaMonica & Marrs, 1976; Zannoni et al., 1976; Zannoni & Marrs, 1981). As expected, the respiratory growth of M6 and its derivatives was sensitive to the cyt bc_1 inhibitor myxothiazol, while that of M7 and its derivatives was resistant to it (Daldal, 1988).

Hüdig and Drews (1981, 1982) isolated from *R. capsulatus* strain 37b4 a cyt *c* oxidase that consisted of a single subunit of M_r 65 000 containing only cyt *b* with an E_{m7} value of 385 ± 15 mV. Later they showed that a *c*-type cyt with an M_r of approximately 12 000 copurified with the cyt *c* oxidase and that this cyt *c* reacted with CO (Hüdig & Drews, 1983). However, they were unable to isolate any mutant lacking this 65-kDa polypeptide from a large collection of Tn5 insertion mutants of strain 37b4, although several mutants affecting cyt *c* oxidase activity were found (Hüdig et al., 1986). More recently, Zannoni et al. (1992) have investigated the electron-transfer chain of a mutant strain of *R. capsulatus* (MT-GS18) that carries chromosomal deletions of cyt c_1 and cyt c_2. They found that additional membrane-bound *c*-type cytochromes are also involved in electron transfer to the cyt *c* oxidase (cyt b_{410}) and suggested that cyt b_{410} may be a *cb*-type cyt *c* oxidase. We describe in this report the purification and characterization of a highly active *cb*-type cyt *c* oxidase (cyt *cb*) from *R. capsulatus* that has properties distinct from the oxidase isolated by Hüdig and Drews (1981). The purified enzyme is composed of three major polypeptides of apparent M_r 45 000, 32 000, and 28 000 containing two electrochemically distinct cyt *c*, one low-spin cyt *b*, and one high-spin cyt *b*. Neither heme A nor heme O is present, and electron paramagnetic resonance (EPR) spectroscopy of the purified enzyme provides evidence that a bound copper atom with properties similar to Cu_A in other cyt *c* oxidases [reviewed in Haltia and Wikström (1992) and Malmström (1993)] is also not present, making cyt *cb* a novel cyt *c* oxidase.

MATERIALS AND METHODS

Bacterial Strains and Growth. *R. capsulatus* strains MT-1131 (wild type), pMT0-404/MT-RBC1 (cyt bc_1 minus strain complemented with the *fbc*FBC operon; Atta-Asafo-Adjei & Daldal, 1991), M7G (C_{ox}^-), and M7G-CBC1 ($bc_1^-C_{ox}^-$) (Daldal, 1988) were grown semiaerobically in MPYE-rich medium in darkness at 35 °C.

Enzyme Purification. pMT0-404/MT-RBC1 cells, washed and suspended in 50 mM Tris-HCl, pH 8, containing 100 mM NaCl, 1 mM phenylmethanesulfonyl fluoride, and 0.5 mM EDTA, were ruptured in a French pressure cell (SLM Aminco, Urbana, IL) at 16 000 psi. Chromatophore membranes were isolated by differential centrifugation and suspended to 10 mg of membrane protein mL^{-1} in the same buffer containing 20% (v/v) glycerol. Dodecyl maltoside was added dropwise to the suspension from a 200 mg mL^{-1} solution to a final concentration of 10 mg mL^{-1}, and the solution was stirred at 4 °C for 45 min. After centrifugation (2.5 h, 4 °C, 130000*g*) the pH of the supernatant was adjusted to 8 and loaded on a Bio-Gel A50 (Bio-Rad Laboratories, Richmond, CA) DEAE anion-exchange column (2.6 cm × 50 cm) that had been equilibrated with 50 mM Tris-HCl, pH 8, 100 mM NaCl, and 20% glycerol. The column was exhaustively washed (approximately 1.5 L) with the same buffer containing 0.1 mg mL^{-1} dodecyl maltoside and eluted with linear 150–400 mM NaCl gradient. A brownish-green band eluted at the beginning of the gradient and had a reduced *minus* oxidized difference spectrum with peaks at 550 and 560 nm and contained cyt *c* oxidase activity. These fractions were pooled and dialyzed overnight against 50 mM Tris-HCl, pH 8, containing 100 mM NaCl and 0.1 mg mL^{-1} dodecyl maltoside. This "enriched preparation" contained no other redox-active groups besides the *b*- and *c*-type cytochromes of the cyt *c* oxidase. Further, this fraction could not catalyze ubiquinol-dependent cyt *c* reduction, indicating that no contaminating cyt bc_1 complex was present. The dialysate was concentrated by ultrafiltration using an XM-50 membrane (MWCO 50 kDa, Amicon, Beverly, MA), loaded onto 8–18% sucrose density gradients (500 mM potassium phosphate, pH 7, with 0.5 mg mL^{-1} dodecyl maltoside), and centrifuged at 150000*g* for 20 h at 4 °C (Finel & Wikström, 1986). A green higher density band and a reddish less dense band were observed on the gradient. The reddish band containing cyt *c* oxidase activity was removed, diluted severalfold with 50 mM Tris-HCl, pH 8, to remove the sucrose, and concentrated using a Centricon-30 miniconcentrator (Amicon, Beverly, MA). It was then applied to an FPLC MonoQ anion-exchange column (Pharmacia LKB Technology) equilibrated with 50 mM Tris-HCl, pH 8, 100 mM NaCl, and 0.1 mg mL^{-1} dodecyl maltoside and eluted with a linear gradient from 100 to 400 mM NaCl. The fractions containing cyt *c* oxidase activity were pooled, concentrated, and stored at −20 °C. Purity of the enzyme was determined by optical spectroscopy and by SDS–PAGE.

SDS–PAGE Analysis. Sodium dodecyl sulfate–polyacrylamide gel electrophoresis was performed by using the Mighty Small II apparatus (Hoefer Scientific Instruments, San Francisco, CA) according to Laemmli (1970) (15% acrylamide) for purified protein, or according to Schägger and von Jagow (1987) using 16.5% acrylamide and 3% cross-linker for membrane samples. Prior to loading, the samples were incubated at 37 °C in the presence of 2% (w/v) SDS and either 100 mM DTT (purified complexes) or 5% (v/v) 2-mercaptoethanol (membrane samples). Gels were stained either for protein with Coomassie Brilliant Blue or with 3,3′,5,5′-tetramethylbenzidine (TMBZ) and H_2O_2 to reveal the heme peroxidase activity as described by Thomas et al. (1976).

Amino Acid Sequence. Amino acid sequence analysis was conducted by automated Edman degradation using an Applied Biosystems Inc. (Foster City, CA) Model 470A sequencer employing manufacturer's programming and chemicals. After SDS–PAGE the proteins were electroblotted to an Immobilon membrane (Millipore Corp., Bedford, MA) using the method of Matsudaira (1987), and the bands were visualized with Coomassie Brilliant Blue and excised. They were either used directly for N-terminal sequencing or digested with trypsin for internal amino acid sequence determination. Products of the trypsin digests were then separated by HPLC, and different peak materials were sequenced directly.

Heme Analysis. Heme extraction was performed as described (Weinstein & Beale, 1983). Briefly, the protein sample was first washed with 5 volumes of ice-cold NH_4OH–acetone (1:9), and it was verified spectroscopically that no heme was present in the basic acetone wash. The supernatant was discarded and the pellet extracted with 5 volumes of ice-cold HCl–acetone (1:9) and centrifuged. The pellet (containing heme C) was air-dried and resuspended in 20% (v/v) pyridine, 50 mM NaOH, and 0.3 mM $K_3Fe(CN)_6$. The supernatant (containing noncovalently bound heme) was dried under a stream of argon gas, and the residue was

suspended in 20% pyridine, 50 mM NaOH, and 0.3 mM K_3-$Fe(CN)_6$. Pyridine hemochrome difference spectra were recorded as described (Berry & Trumpower, 1987) using $\epsilon_{549-535}$ = 23.97 mM^{-1} cm^{-1} for heme C and $\epsilon_{556-540}$ = 22.98 mM^{-1} cm^{-1} for protoheme. Alternatively, hemes were re-extracted from the HCl–acetone with diethyl ether and washed with water for HPLC analysis.

HPLC analysis of the noncovalently bound hemes was performed essentially as described (Puustinen & Wikström, 1991) and according to Dr. T. Mogi (personal communication). Briefly, ether-extracted hemes were dried under a stream of Ar gas, suspended in ethanol–acetic acid–water (70:17:13), and separated on an Altrex Ultrasphere ODS reverse-phase column (4.6 mm × 250 mm, 5-μm spherical 80-Å pore size) using the same solvent and a flow rate of 0.5 mL min^{-1} with a Spectra Physics SP8700 XR system. Heme-containing fractions were detected by monitoring the absorption at 402 nm using a Spectra Physics SP8440 variable-wavelength detector. Sperm whale myoglobin and aa_3-type cyt *c* oxidase from beef heart (a kind gift from Dr. T. Ohnishi) (Yu et al., 1975) were treated in the same manner and used as controls to determine the retention time of protoheme and heme A using this column and solvent system.

CO Difference Spectra. Purified cyt *cb* was made anaerobic in a stoppered cuvette by purging with Ar gas and then reduced with a concentrated solution of sodium dithionite. An absorption spectrum was recorded and stored on a Hitachi U3210 spectrophotometer. The sample was allowed to equilibrate for approximately 1 h in the dark to ensure complete reduction, and a second spectrum was recorded. CO gas was then slowly bubbled through the sample for several minutes in the dark, and before recording the spectrum of the CO-bound form, additional dithionite was added. The reduced plus CO *minus* reduced difference spectrum was obtained by subtraction of these two spectra. As a control the same manipulations were performed on myoglobin, and the difference spectrum obtained was indistinguishable from the literature (Wood, 1984).

Redox Titrations. Anaerobic potentiometric titrations of the heme groups were performed as outlined by Dutton (1978) using 50 μM 2,5-dihydroxy-1,4-benzoquinone, 25 μM 1,4-benzoquinone, 70 μM 2,3,5,6-tetramethyl-*p*-phenylenediamine, 25 μM 1,2-naphthoquinone, 20 μM *N*-methyldibenzopyrazine methosulfate (PMS), 20 μM *N*-ethyldibenzopyrazine ethosulfate (PES), and 25 μM duroquinone as redox mediators. E_m values were obtained after fitting normalized absorbance differences ($A_{550} - A_{540}$ for cyt *c* and $A_{560} - A_{570}$ for cyt *b*) to either single or multiple theoretical $n = 1$ Nernst equations.

Catalytic Activity. Cyt *c* oxidase activity was measured by monitoring the oxidation of cyt *c* [either equine or *R. capsulatus* cyt c_2 (a kind gift from Dr. R. Prince)] at 550 nm in a stirred cuvette (thermostated at 25 °C) containing 50 mM Tris-HCl, pH 8, 0.1 mg mL^{-1} dodecyl maltoside, 5 μM myxothiazol, and 40 μM prereduced cyt *c*. Cyt *c* was prereduced by the addition of a small amount of solid sodium dithionite to a concentrated protein solution followed by passage over a Sephadex G-10 size-exclusion column. Oxygen consumption was measured polarographically (25 °C) with a Clark-type oxygen electrode (courtesy of Dr. T. Ohnishi) using an assay mixture containing 100 μM *N,N,N′,N′*-tetramethyl-*p*-phenylenediamine (TMPD), 2 mM ascorbate, 0.1 mg mL^{-1} dodecyl maltoside, and 5 μM myxothiazol in 50 mM Tris-HCl, pH 8, and 100 mM NaCl. Cyanide-insensitive cyt *c* oxidation and O_2 consumption were subtracted from the traces to determine the final rates.

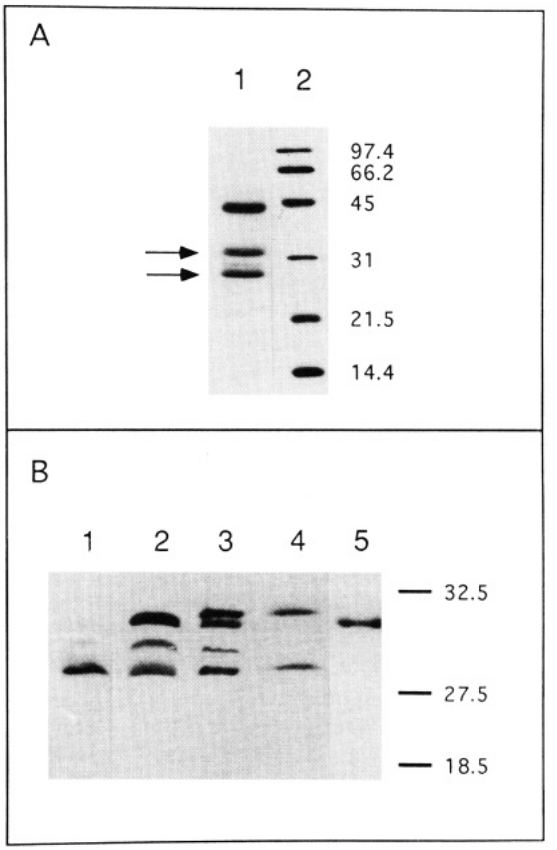

FIGURE 1: (A) SDS–PAGE (15% acrylamide) of purified cyt *cb* (lane 1). Lane 2 shows molecular weight markers from Bio-Rad. Cyt *cb* (5 μg of protein) was heated to 37 °C in the presence of 2% SDS and 100 mM DTT prior to loading on the gel. (B) SDS–PAGE (16.5% acrylamide) of chromatophore membranes (300 μg of protein) of *R. capsulatus* wild-type strains MT-1131 (lane 3), M7G (lane 2), and M7G-CBC1 (lane 1) and purified cyt *cb* (30 μg of protein, lane 4) and cyt bc_1 complexes (30 μg of protein, lane 5). The gel was stained for heme using TMBZ and H_2O_2. The positions of the prestained standards are shown to the right.

Electron Paramagnetic Spectroscopy. Spectra of air-oxidized cyt *cb* and beef heart cyt aa_3 were obtained on a Bruker ESP 300E spectrometer equipped with a variable-temperature continuous-flow helium cryostat (Oxford Instruments ESR 900) (courtesy of Dr. P. L. Dutton). The spectra were recorded at 10 and 77 K at a power setting of 4 mW, a microwave frequency of 9.44 GHz, and modulation amplitude of 10.05 G.

Chemicals. 1,2-Naphthoquinone, 2,3,5,6-tetramethyl-*p*-phenylenediamine, duroquinone, and 1,4-naphthoquinone were purchased from Aldrich Chemical Co. (Milwaukee, WI). Equine cyt *c*, TMPD, TMBZ, PMS, PES, 2,5-dihydroxy-1,4-benzoquinone, 1,4-benzoquinone, and myoglobin were from Sigma Chemical Co. (St. Louis, MO). Myxothiazol was purchased from Boehringer-Mannheim Biochemicals. *n*-Dodecyl β-D-maltoside (dodecyl maltoside) was from Anatrace (Maumee, OH). All other chemicals were reagent grade and were purchased from commercial sources.

RESULTS

Purification and Subunit Composition of R. capsulatus Cyt c Oxidase. SDS–PAGE analysis of the purified active cyt *c* oxidase (cyt *cb*) indicated that it consists of three major polypeptides with apparent molecular masses of 45, 32, and 28 kDa (Figure 1A). The two smaller subunits (i.e., 32 and 28 kDa) can also be visualized by their heme peroxidase activity using TMBZ (Figure 1B, lane 4), indicating that they are *c*-type cytochromes. Using the Schägger-type SDS–PAGE

Table 1: Partial Amino Acid Sequences Obtained from the Three Subunits of Cyt *cb* of *R. capsulatus*

subunit	amino terminal	internal
45 kDa	xIKEVNxxTxLRxQ	xxxAFYAPATSxIE
		DLLGITL
32 kDa		ATVMPSxSxAADGAxP
		AVEDKLVATDLTAIAADPELVT
		AVASYVHSLGGGS
		LMATDLTAIAA
28 kDa	xIMDKxxVLEK-NATLLLIF	VSTDALVGVPYYDAPFQAN
		YHDAWHVEHLSNPQxSGPF
		ADFVAQADPNADSATxAN

system (Schägger & von Jagow, 1987), four distinct *c*-type cytochromes are visible in chromatophore membranes of the wild-type *R. capsulatus* strain MT-1131 grown semiaerobically in MPYE-rich medium (Figure 1B, lane 3). These cytochromes have apparent molecular masses of approximately 32, 31, 29, and 28 kDa. Neither an alkaline (pH 11) wash nor treatment with chaotrophic agents (up to 1 M NaBr) resulted in the dissociation of any of these four proteins from the membrane fraction (data not shown), indicating that all are integral membrane proteins. Of these cytochromes the 31-kDa protein is identified as cyt c_1 by comparison with purified cyt bc_1 complex (Figure 1B, lane 5), and by using mutants lacking it (Jenney et al., 1994). The 29-kDa protein correlates with the newly discovered membrane-associated cyt c_y (Jenney & Daldal, 1993; Myllykallio, Jenney, and Daldal, unpublished), and the two remaining 32- and 28-kDa cytochromes correspond to the heme C-containing subunits of the purified cyt *cb* (Figure 1B, lane 4). Chromatophore membranes of the mutants M7G (C_{ox}^-) (Figure 1B, lane 2) and M7G-CBC1 ($bc_1^-C_{ox}^-$) (Figure 1B, lane 1) known to lack cyt *c* oxidase activity (LaMonica & Marrs, 1976; Zannoni, et al., 1976; Daldal, 1988) are also devoid of the 32-kDa cyt *c*. Further, M7G-CBC1 also lacks cytochromes c_1 and c_y and contains mainly the 28-kDa cyt *c* subunit of cyt *cb* (Figure 1B, lane 4). The absence cyt c_y in cyt bc_1-minus mutants grown on MPYE-rich medium has been described recently (Jenney et al., 1994).

Catalytic Activity of the Purified Cyt c Oxidase. The purified *R. capsulatus* cyt *c* oxidase catalyzes the oxidation of ferrocyt *c* (equine and purified *R. capsulatus* cyt c_2) and the reduction of O_2 as monitored by oxygen uptake using TMPD/ascorbate as electron donors, and the final preparation consumed oxygen at a rate of 300 mol of O_2 s^{-1} (mol of heme C)$^{-1}$ [which corresponds to a turnover number of 600 s^{-1} considering the stoichiometry of 2 heme C per enzyme (see below)]. Both cyt *c* oxidation and O_2 uptake activities are inhibited by low concentrations of cyanide (25 μM KCN for 100% inhibition in a typical assay). The addition of the ubihydroquinone analog, 2,3-dimethoxy-5-decyl-6-methylbenzohydroquinone (DBH), did not elicit O_2 uptake, verifying that the enzyme is not a quinol oxidase.

Partial N-Terminal and Internal Peptide Sequences of the Three Subunits of the Purified Cyt c Oxidase. Table 1 shows the different N-terminal and internal peptide amino acid sequences obtained from the 45-, 32-, and 28-kDa subunits of the purified cyt *cb*. A search of the various sequence data banks with these peptides revealed significant homologies to the gene products of the *fix*N, -O, and -P genes of both *Bradyrhizobium japonicum* (Preisig et al., 1993) and *Rhizobium meliloti* (GenBank Accession Number Z21854; Daveran-Mingot, 1988) as shown in Figure 2. There is also strong homology between the N-terminal amino acid sequence of the 28-kDa cyt *c* subunit from *R. capsulatus* and that of a similar enzyme purified from *Rhodobacter sphaeroides* [see the preceding paper in this issue (Garćia-Horsman et al., 1994)].

Characterization of the Purified Cyt c Oxidase Enzyme. (A) Optical Absorption Spectrum. The room temperature electronic absorption spectrum of the ascorbate-reduced purified cyt *cb* of *R. capsulatus* is shown in Figure 3A. The Sorêt maximum is at 418 nm with asymmetry on the long-wavelength side, and there are two distinct peaks in the α-band region with maxima near 550 and 560 nm. The ascorbate-reduced *minus* ferricyanide-oxidized difference spectrum is also shown in the inset of the figure. While the features in the α-band region indicate that the purified enzyme contains both *c*- and *b*-type cytochromes, the absence of any absorbance near 600 nm suggests that it does not contain any cyt *a*.

(B) Carbon Monoxide Binding. Figure 3B shows the dithionite-reduced + CO *minus* dithionite-reduced difference spectrum of cyt *cb* with maxima at 415, 535, and 565 nm and troughs at 427 and 553 nm, a pattern typical of CO binding to a high-spin cyt *b* (Wood, 1984). Note that the spectral features of the CO difference spectrum of this enzyme are blue shifted with respect to those observed with CO-bound myoglobin (peaks: 422, 536, and 580 nm; troughs: 438 and 558 nm), but they are quite similar to the features observed

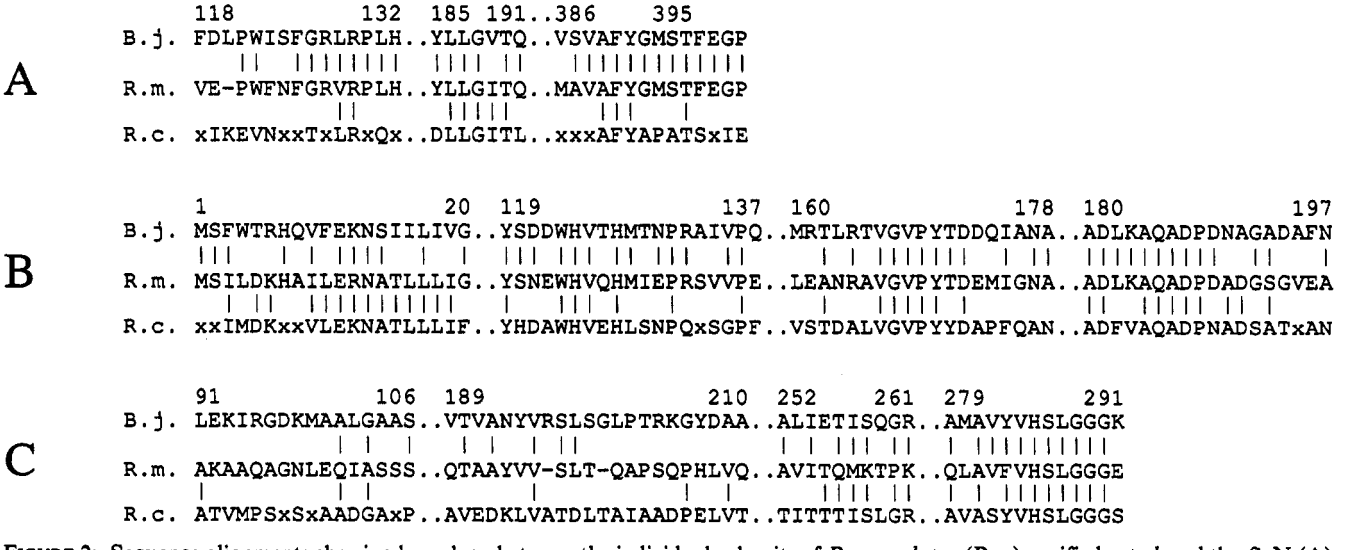

FIGURE 2: Sequence alignments showing homology between the individual subunits of *R. capsulatus* (R.c.) purified cyt *cb* and the *fix*N (A), *fix*O (B), and *fix*P (C) gene products of *B. japonicum* (B.j.; Preisig et al., 1993) and *R. meliloti* (R.m.; Daveran-Mingot, 1988). Lines between the various sequences represent identities of the residues from *R. capsulatus* with at least one of the other sequences.

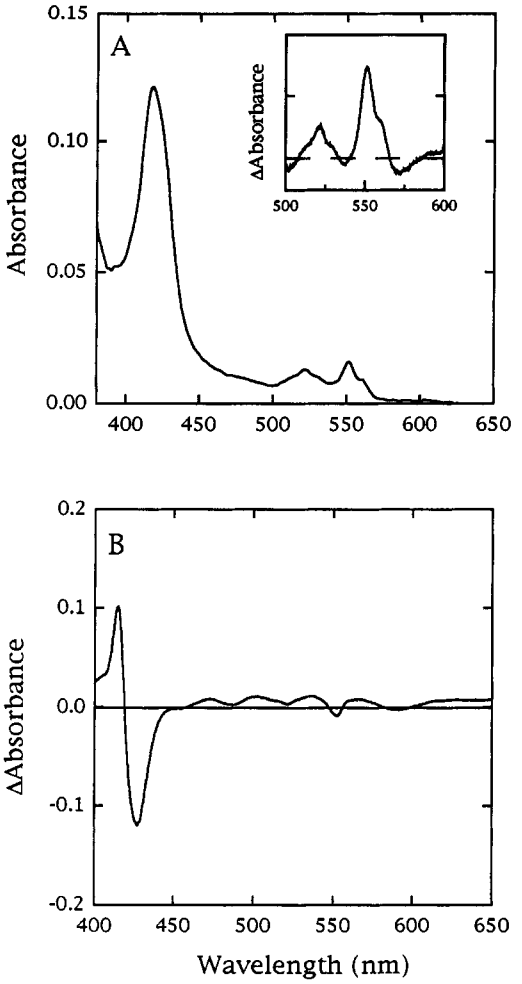

FIGURE 3: (A) Optical absorption spectrum and ascorbate/PMS-reduced *minus* ferricyanide-oxidized difference spectrum (inset) of purified cyt *cb*. The complex was in 50 mM Tris-HCl, pH 8, containing 100 mM NaCl, 1 mM ascorbate, and 0.1 mg mL^{-1} dodecyl maltoside. (B) CO difference spectrum (reduced + CO *minus* reduced) of purified cyt *cb*. See Materials and Methods for details.

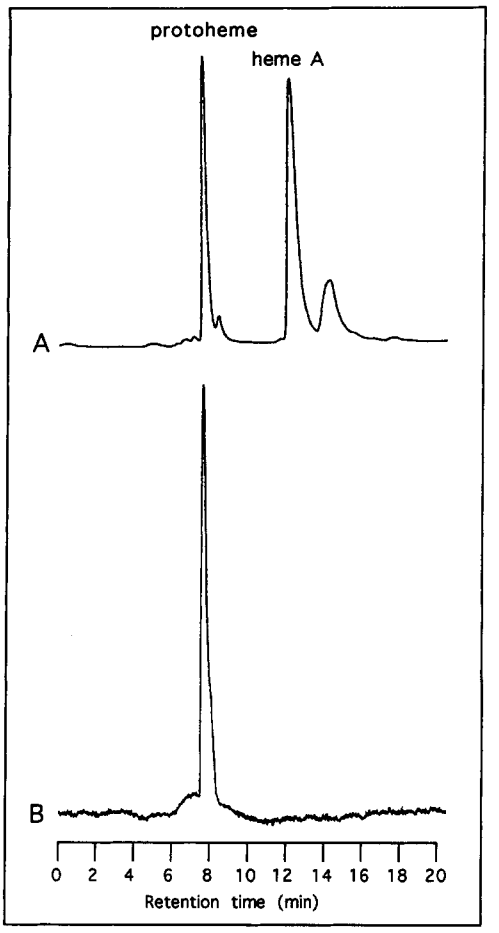

FIGURE 4: Analytical HPLC of the noncovalently bound hemes from myoglobin and bovine cyt aa_3 (A) and cyt *cb* (B). The detection wavelength was 402 nm, and the experimental conditions are described in Materials and Methods.

in the CO difference spectrum of purified *Escherichia coli* cyt *bo* ubiquinol oxidase (Puustinen & Wikström, 1991). The spectroscopic data shown in Figure 3 (panels A and B together) indicate that the purified cyt *c* oxidase of *R. capsulatus* contains both a low-spin and high-spin cyt *b* and is therefore a *cb*-type cyt *c* oxidase.

Heme Analysis. Hemes were extracted from purified cyt *cb* with HCl–acetone as described in Materials and Methods, and their nature and amount were characterized by pyridine hemochrome analysis and analytical HPLC. As expected, the pyridine hemochrome difference spectrum (data not shown) of the protein-associated heme revealed an α-peak at 549 nm, identifying it as heme C (Berry & Trumpower, 1987). Using the known difference extinction coefficient for heme C in alkaline pyridine a reduced *minus* oxidized difference extinction coefficient ($\epsilon_{550-540}$) for cyt *c* in cyt *cb* of 49 mM^{-1} cm^{-1} heme^{-1} was calculated. This corresponds to an $\epsilon_{550-540}$ of 24.5 mM^{-1} cm^{-1} for the enzyme considering a stoichiometry of 2 heme C per enzyme complex (see below). On the other hand, the noncovalently bound hemes had an α-peak at 555 nm in alkaline pyridine, and this confirmed that heme A (with an α-peak at 589 nm; Falk, 1964) was not present. The spectral data suggested that the only noncovalently attached heme in this cyt *c* oxidase may be protoheme (heme B) since heme B has an α-peak at 556 nm in alkaline pyridine (Falk, 1964) while heme O has a slightly blue-shifted α-peak at 552 nm in alkaline pyridine (Puustinen & Wikström, 1991). This was further verified by analytical HPLC. Both heme A and heme O are more hydrophobic than protoheme due to the presence of a farnesylhydroxyethyl side chain (Wu et al., 1992); therefore, the retention time of these species on a reverse-phase column is longer than that of protoheme (Puustinen & Wikström, 1991). Protoheme and heme A were extracted from myoglobin and beef heart aa_3-type cyt *c* oxidase, respectively, run individually (not shown), and mixed (Figure 4A) through the C18 column. The separation of the mixture resulted in two clearly resolved major peaks in the elution pattern. The nature of the two minor peaks is unknown, but they may correspond to impurities or aggregation products. On the other hand, only one type of noncovalently bound heme was detected in the extract of purified cyt *cb*, and its retention time corresponds to that of protoheme (Figure 4B). If heme O were present in this sample, it would be expected to be retained slightly longer than heme A since heme O is more hydrophobic (Puustinen & Wikström, 1991).

Using the extinction coefficients for heme C and protoheme coordinated by pyridine (Berry & Trumpower, 1987), it was calculated that cyt *cb* contains approximately 1 mol of heme C to 1 mol of protoheme. Thus the overall chemical and spectral data indicate that the purified *cb*-type cyt *c* oxidase of *R. capsulatus* contains at least two hemes C, one high-spin heme B and one low-spin heme B.

Electron Paramagnetic Resonance. X-band EPR spectra of *R. capsulatus* cyt *c* oxidase taken at both 10 and 77 K are shown in Figure 5, panels A and B, respectively (upper spectra). For comparison, the spectra of the bovine aa_3-type cyt *c* oxidase are also shown (lower spectra). At 10 K, resonances due to

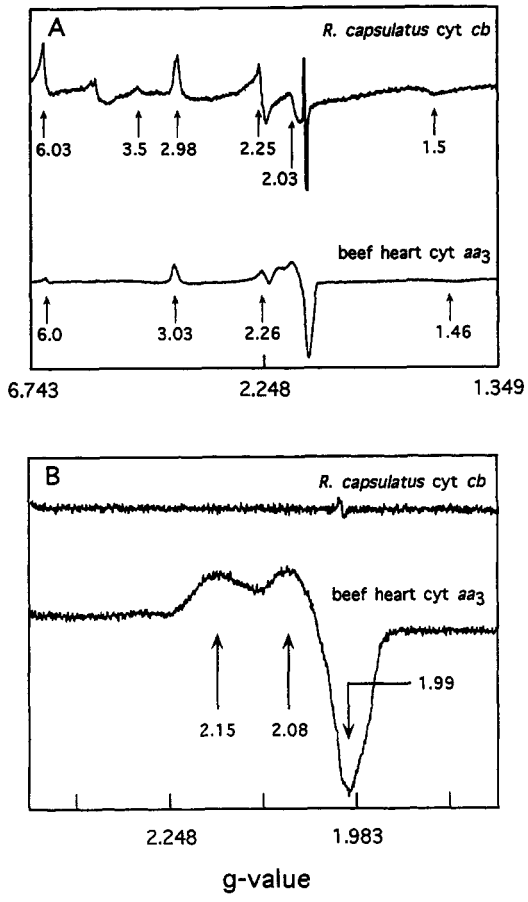

FIGURE 5: X-band EPR spectra of cyt *cb* from *R. capsulatus* and bovine cyt aa_3 taken at 10 (A) and 77 K (B). EPR conditions are described in the text, and the *g* values are shown in the figure.

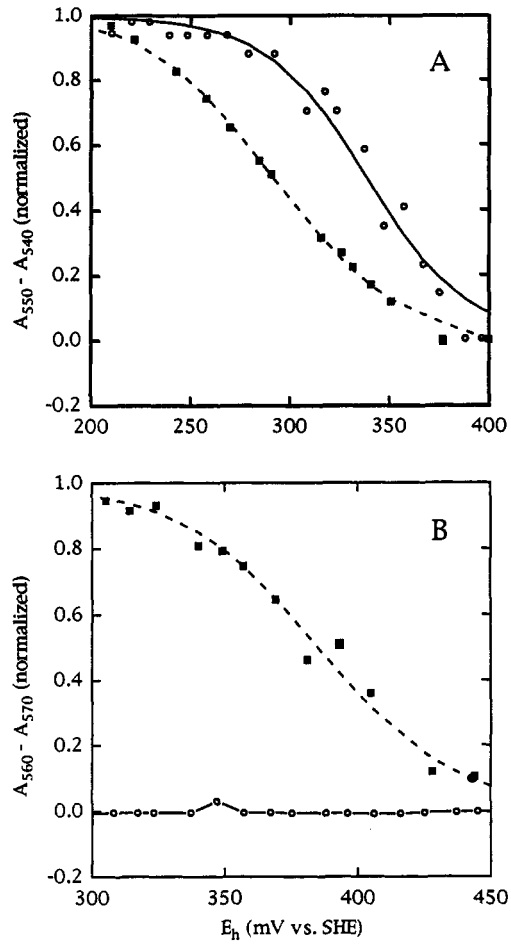

FIGURE 6: Oxidation–reduction midpoint potential titrations of cyt *c* (A) and cyt *b* (B). Each panel shows data from an "enriched preparation" of cyt *cb* (filled squares) and membranes from the C_{ox}^- strain M7G-CBC1 (open circles). The solubilized protein was in 50 mM Tris-HCl, pH 7, containing 100 mM NaCl and 0.1 mg mL^{-1} dodecyl maltoside and redox mediators (listed in Materials and Methods). Chromatophore membranes were in 50 mM MOPS, pH 7, containing 100 mM KCl and redox mediators. The lines are fits of the data to theoretical $n = 1$ Nernst equations with midpoint potentials given in the text.

high-spin ferric hemes with axial symmetry (with *g* values of 6.03 and 2.03 in *R. capsulatus* enzyme) and due to low-spin ferric hemes with rhombic symmetry (with g_z values of 3.5 and 2.98; $g_y = 2.25$ and $g_x = 1.5$ in *R. capsulatus* enzyme) are apparent (Figure 5A) (Palmer, 1983). The signal seen at $g = 2.005$ (line width of 12 G) is due to a free radical of unknown origin while that seen around 4.3 is due to adventitious Fe^{3+}. Spectra recorded at various power intensities (ranging from 0.1 to 63.6 mW) demonstrated that 4 mW was not saturating for any of the signals (data not shown). The spectrum of bovine cyt aa_3 also shows resonances from both a high-spin ferricytochrome (heme a_3, $g = 6.00$) and a low-spin ferricytochrome (heme *a*, $g_z = 3.03$, $g_y = 2.26$, and $g_x = 1.46$). In addition, the well-known Cu_A signal is observed, with *g* values of 2.15, 2.08, and 1.99 [reviewed in Wikström et al. (1981)]. Figure 5B shows the spectra recorded at 77 K, where the heme signals are undetectable and only the Cu_A resonances are observed. It is clear from these spectra that a species with spectral properties similar to Cu_A in cyt aa_3 is not present in the purified active cyt *c* oxidase from *R. capsulatus*. It is unlikely that the absence of Cu_A in cyt *cb* is due to the loss of a subunit(s) during enzyme preparation since the purified complex is highly active as both a cyt *c* oxidase and an "O_2 reductase". Comparison of the EPR spectra of the bovine and the bacterial cyt *c* oxidases indicates that in the $g = 2$ region the *R. capsulatus* cyt *c* oxidase more closely resembles that of the cyt *bo* quinol oxidase of *E. coli* (which does not contain Cu_A) than bovine cyt aa_3 (Puustinen et al., 1991).

Determination of the Redox Midpoint Potentials of the c and b Cytochromes Associated with R. capsulatus Cyt c Oxidase. Equilibrium potentiometric titrations of an "enriched preparation" of *R. capsulatus* cyt *cb* (see Materials and Methods) indicated the presence of a low-spin cyt *b* with a redox midpoint potential (E_{m7}) of about 385 mV (Figure 6B). On the other hand, it was necessary to use two $n = 1$ Nernst equations to satisfactorily fit the data obtained for cyt *c* titrations (Figure 6A). Each component contributes equally to the fit but with E_{m7} values of 265 and 320 mV. Thus the complex contains at least two electrochemically distinct cyt *c*, henceforth referred to as cyt c_{265} and cyt c_{320}. These values are quite similar to those (265 and 354 mV) obtained by Zannoni et al. (1992) using membranes of *R. capsulatus* strain MT-GS18 which is devoid of both cytochromes c_1 and c_2.

It has previously been demonstrated that the *R. capsulatus* mutant M7 defective in the cyt *c* oxidase activity lacks the cyt b_{410} (LaMonica & Marrs, 1976; Zannoni et al., 1976). Analysis of its "green" derivative M7G (C_{ox}^-, *crt*D121) by SDS–PAGE indicated that it lacks the 32-kDa cyt *c* as shown in Figure 1, lane 3. Further, its cyt bc_1-minus derivative M7G-CBC1 (Daldal, 1988) grown in MPYE-rich medium also lacks the two other membrane-associated cyts c_1 and c_y (Figure 1B, lane 1). This observation made it possible to determine the redox midpoint potential of the remaining 28-kDa molecular mass cyt *c*. Titration of chromatophore membranes isolated from M7G-CBC1 revealed that the E_{m7} of the cyt *c* present was about 320 mV and that the cyt b_{410} and cyt c_{265} were

absent (Figure 5). Therefore, the 28-kDa cyt *c* has an E_{m7} value of approximately 320 mV while the larger 32-kDa cyt *c* has an E_{m7} value of about 265 mV.

DISCUSSION

We describe here the purification and biochemical characterization of a highly active *cb*-type cyt *c* oxidase (cyt *cb*) from cytoplasmic membranes of aerobically grown *R. capsulatus*. The enzyme is similar to cyt *c* oxidases purified from other prokaryotes, namely, *Pseudomonas aeruginosa* (Matsushita et al., 1982), *Rhodopseudomonas palustris* (King & Drews, 1976), *Azotobacter vinelandii* (Yang & Jurtshuk, 1978), *Methylophilus methyltrophus* (Froud & Anthony, 1984), *Acetobacter methanolicus* (Elliot & Anthony, 1988), and *R. sphaeroides* (Garćia-Horsman et al., 1992, 1994). These cyt *c* oxidases contain *b*- and *c*-type cytochromes, and Froud and Anthony (1984) suggested that these enzymes be called cyt *cb* analogous to cyt aa_3. Interestingly, these cyt *cb* oxidases tend to be common in methylotrophic bacteria, and their presence in those species seems to depend upon the availability of carbon [reviewed in Anthony (1992)]. In contrast to the closely related bacterium *R. sphaeroides*, heme A has not been detected in membranes of *R. capsulatus* (Klemme & Schlegel, 1969; Zannoni et al., 1974); thus no cyt aa_3 is present in the latter bacterium, and the only known cyt *c* oxidase in this organism is the "cyt b_{410}" (Zannoni et al., 1976; LaMonica & Marrs, 1976). Isolation of the genes complementing the *R. capsulatus* mutant M7 lacking "cyt b_{410}" and comparison of the deduced amino acid sequences with those obtained from the subunits of cyt *cb* should indicate whether these two cyt *c* oxidases are identical.

Recently, Preisig et al. (1993) have described a gene cluster (*fix*NOQP) in *B. japonicum* that apparently encodes a cyt *c* oxidase utilized under microaerophilic growth conditions. Similar genes have previously been isolated and sequenced from *R. meliloti* (Daveran-Mingot, 1988; D. Kahn, personal communication). The deduced amino acid sequences from these genes suggested that the enzyme consists of 3–4 polypeptides of M_r's 61 000 (FixN), 27 000 (FixO), 6000 (FixQ), and 31 000 (FixP). FixN is homologous to subunit I of other terminal oxidases and could accommodate Cu and heme, making it a member of the superfamily of terminal oxidases containing a binuclear center at the oxygen reduction site (Saraste, 1990; Haltia & Wikström, 1992; Babcock & Wikström, 1992). FixO and FixP contain one and two heme C binding domains, respectively, and are apparently membrane-associated *c*-type cytochromes. The overall similarity between cyt *cb* from *R. capsulatus* described here and the expected complexes from *B. japonicum* and *R. meliloti* is striking. In particular, the partial peptide sequences currently available for the individual subunits of *R. capsulatus* cyt *cb* (Table 1) show strong homology with FixN, FixO, and FixP proteins (Figure 2), suggesting that they indeed represent similar oxidases. However, a major difference between the *R. capsulatus* and *B. japonicum* complexes seems to be the number of heme cofactors. Pyridine hemochrome difference spectra suggest a heme C:heme B ratio of 1 for *R. capsulatus* cyt *cb*, but the amino acid sequences deduced from the *fixNOQP* cluster indicate that it may be 3:2. The resolution of this difference should await the availability of the corresponding gene cluster from *R. capsulatus*.

The members of the superfamily of proton-translocating terminal oxidases, including various quinol oxidases and both mitochondrial and prokaryotic cyt *c* oxidases, share several common structural and functional properties (Saraste, 1990; Babcock & Wikström, 1992; Hosler et al., 1993). They are typified by having a heme/copper binuclear center and a low-spin heme all bound to a single well-conserved subunit (so-called subunit I). The Cu (Cu_B) at the binuclear center is antiferromagnetically coupled to the high-spin heme forming the site of O_2 chemistry. The cyt *c* oxidases contain a second tightly bound Cu (Cu_A) located in subunit II, and it has been suggested that the presence of this metal center is necessary for the oxidation of cyt *c* (Haltia & Wikström, 1992). It is at this point that the cyt *c* and quinol oxidases diverge since quinol oxidases only contain Cu_B and no Cu_A. The subunit II analog of quinol oxidases does not contain a Cu_A binding motif (two cysteines and a histidine separated from one another by three residues and a histidine located about forty residues away toward the N-terminus; Holm et al., 1987) (Chepuri et al., 1990), and EPR data have confirmed that *E. coli* cyt *bo* quinol oxidase does not contain Cu_A (Puustinen & Wikström, 1991).

Although we have no direct physical evidence for the presence of a binuclear site in cyt *cb* of *R. capsulatus*, several indirect lines of evidence suggest that it may be present. First, Shapleigh et al. (1992) have shown that a second heme/Cu cyt *c* oxidase containing a binuclear center that does not contain heme A is present in the closely related bacterium *R. sphaeroides*. Recently, Gennis and co-workers have demonstrated that this second binuclear center-containing cyt *c* oxidase is the cyt *cb* in that organism [preceding paper in this issue (Garćia-Horsman et al., 1994)]. The enzymes from the two organisms are very similar and have many identical properties, including the strong N-terminal amino acid sequence homology between the two small cyt *c* subunits of the complex [Figure 2 and Garćia-Horsman et al., (1994)]. Second, the sequence homology between the 45-kDa subunit of cyt *cb* and the subunit I analog FixN of *B. japonicum* and *R. meliloti* (Figure 2) suggests that cyt *cb* of *R. capsulatus* may also belong to the superfamily of terminal oxidases; however, this needs direct experimental confirmation.

Two distinct aspects of the cofactor arrangement of cyt *cb* make it a novel member of the cyt *c* oxidase subgroup of the superfamily of terminal oxidases. First, while the site of the low-spin heme of the terminal oxidases seems to be nondiscriminating as to the type of heme (Puustinen et al., 1992), the heme at the binuclear center appears to always contain a hydroxyethylfarnesyl side chain (i.e., heme A or O). Thus, assuming that *R. capsulatus* cyt *cb* contains a binuclear center like its *R. sphaeroides* counterpart, the alkyl chain is unnecessary for O_2 reduction since neither heme A nor heme O is present in cyt *cb*. Second, the EPR data presented above support the conclusion that cyt *cb* from *R. capsulatus* does not contain a Cu with properties similar to Cu_A, and indeed, an inspection of the *B. japonicum* and *R. meliloti fix*NOQP sequences does not reveal a consensus Cu_A binding motif. Perhaps, the presence of two tightly bound cytochromes *c* in these cyt *c* oxidases in some way obviates the requirement of an intervening Cu for the oxidation of cyt *c*.

The necessity of Cu_A in the cyt *c* oxidases may partly be due to the cellular location of the electron donor, cyt *c* (Puustinen, 1993). Topological models of subunit II predict that its Cu_A binding region projects into the aqueous phase (i.e., the periplasm or intermembrane space of mitochondria) and that its cyt *c* binding domain consists of negatively charged amino acid residues in the vicinity of the Cu (Holm et al., 1987). This arrangement is unnecessary in quinol oxidases since quinol is buried in the lipid bilayer and could more easily interact with the low-spin heme bound to transmembrane helices of subunit I. Both of the *c*-type cytochromes of cyt *cb*, FixO and FixP, are predicted to be anchored to the

membrane by a hydrophobic domain near their respective N-termini (Preisig et al., 1993). This configuration would leave their heme binding domains in a more hydrophilic portion of the protein extending into the aqueous phase (similar to other membrane-associated cyt *c* like cyt c_1 and the cyt *c* subunit of the photosynthetic reaction center), and able to interact with the soluble cyt c_2. Thus it may not be so surprising that a membrane-associated cyt *c* can functionally replace Cu_A.

Finally, it should be noted that although *R. capsulatus* cyt c_2 can be oxidized by cyt *cb in vitro*, neither the nature of the preferred electron carrier(s) to it *in vivo* nor the pathway of electron transfer through cyt *cb* is currently known. Presumably, one of the cyt *c* subunits of cyt *cb* is the initial electron acceptor from cyt c_2 or from other functionally similar electron carriers such as cyt c_y (Jenney et al., 1994). From a purely energetic standpoint cyt c_{320} would be the likely candidate as the initial acceptor since electron transfer from cyt c_2 (E_{m7} = 320 mV) to cyt c_{265} is unfavorable. Perhaps cyt c_{265} is necessary for an as yet unknown pathway. While many other possibilities exist, certainly future experiments will be geared to elucidate the pathways of electron transfer in this novel cyt *c* oxidase.

ACKNOWLEDGMENT

We thank Drs. T. Mogi for providing us with the protocol for the HPLC analysis of hemes, T. Ohnishi for the kind gift of beef heart aa_3-type cyt *c* oxidase, and R. B. Gennis for providing us with unpublished data from his laboratory. We also acknowledge the invaluable help of Dr. Dan E. Robertson with the EPR as well as many helpful discussions.

REFERENCES

Anthony, C. (1992) *Biochim. Biophys. Acta 1099*, 1–15.
Atta-Asafo-Adjei, E., & Daldal, F. (1991) *Proc. Natl. Acad. Sci. U.S.A. 88*, 492–496.
Babcock, G. T., & Wikström, M. (1992) *Nature 356*, 301–309.
Baccarini-Melandri, A., & Zannoni, D. (1978) *J. Bioenerg. Biomembr. 10*, 109–138.
Baccarini-Melandri, A., Zannoni, D., & Melandri, B. A. (1973) *Biochim. Biophys. Acta 314*, 298–311.
Berry, E. A., & Trumpower, B. L. (1987) *Anal. Biochem. 161*, 1–15.
Chepuri, V., Lemieux, L., Au, D. C.-T., & Gennis, R. B. (1990) *J. Biol. Chem. 265*, 11185–11192.
Cramer, W. A., & Knaff, D. B. (1990) in *Energy Transduction in Biological Membranes* (Cantor, C. R., Ed.) Springer-Verlag, New York.
Daldal, F. (1988) *J. Bacteriol. 170*, 2388–2391.
Daveran-Mingot, M.-L. (1988) Ph.D. Thesis, Université Paul Sebatier de Toulouse, France.
Dutton, P. L. (1978) *Methods Enzymol. 54*, 411–435.
Dutton, P. L. (1986) in *Encyclopedia of Plant Physiology* (Staelin, A., & Arntzen, C. J., Eds.) Vol. 19, pp 197–237, Springer Verlag, New York.
Elliot, E. J., & Anthony, C. (1988) *J. Gen. Microbiol. 134*, 369–377.
Ferguson, S. J., Jackson, J. B., & McEwan, A. G. (1987) *FEMS Microbiol. Rev. 46*, 117–143.
Finel, M., & Wikström, M. (1986) *Biochim. Biophys. Acta 851*, 99–108.
Froud, S. J., & Anthony, C. (1984) *J. Gen. Microbiol. 130*, 2201–2212.
García-Horsman, A., Shapleigh, J. P., & Gennis, R. B. (1992) *Biochim. Biophys. Acta* (EBEC Reports), *7*, II–80.
García-Horsman, J. A., Berry, E., Shapleigh, J. P., Alben, J. O., & Gennis, R. B. (1994) *Biochemistry* (preceding paper in this issue).
Haltia, T., & Wikström, M. (1992) in *Molecular Mechanisms in Bioenergetics* (Ernster, L., Ed.) pp 217–239, Elsevier Science Publishers, Amsterdam.
Holm, L., Saraste, M., & Wikström, M. (1987) *EMBO J. 6*, 2819–2823.
Hosler, J. P., Ferguson-Miller, S., Calhoun, M. W., Thomas, J. W., Hill, J., Lemieux, L., Ma, J., Georgiou, C., Fetter, J., Shapleigh, J., Tecklenburg, M. M. J., Babcock, G. T., & Gennis, R. B. (1993) *J. Bioenerg. Biomembr. 25*, 121–136.
Hüdig, H., & Drews, G. (1981) *Z. Naturforsch. 37c*, 193–198.
Hüdig, H., & Drews, G. (1982) *FEBS Lett. 146*, 389–392.
Hüdig, H., & Drews, G. (1983) *FEBS Lett. 152*, 251–255.
Hüdig, H., Kaufmann, N., & Drews, G. (1986) *Arch. Microbiol. 145*, 378–385.
Jenney, F. E., & Daldal, F. (1993) *EMBO J. 12*, 1283–1292.
Jenney, F. E., Prince, R., & Daldal, F. (1994) *Biochemistry* (in press).
Jurtshuk, P., Müller, T. M., & Wong, T. Y. (1981) *Biochim. Biophys. Acta 637*, 374–382.
King, M. T., & Drews, G. (1976) *Eur. J. Biochem. 68*, 5–12.
Klemme, J. H., & Schlegel, H. G. (1969) *Arch. Microbiol. 68*, 326–354.
Laemmli, U. K. (1970) *Nature 227*, 680.
LaMonica, R., & Marrs, B. L. (1976) *Biochim. Biophys. Acta 423*, 431–439.
Malmström, B. (1993) *Chem. Rev. 90*, 1247–1260.
Marrs, B., & Gest, H. (1973) *J. Bacteriol. 114*, 1045–1051.
Matsudaira, P. (1987) *J. Biol. Chem. 262*, 10035–10038.
Matsushita, K., Shinagawa, E., Adachi, O., & Ameyamam, M. (1982) *FEBS Lett. 139*, 255–258.
McEwan, A. G., Greenfield, A. J., Wetzstein, H. G., Jackson, J. B., & Ferguson, S. J. (1985) *J. Bacteriol. 164*, 823–830.
Palmer, G. (1983) in *Iron Porphyrins* (Lever, H. B. P., & Gray, H. B., Eds.) Vol. II, pp 43–88, Addison-Wesley Publishers.
Preisig, O., Anthamatten, D., & Hennecke, H. (1993) *Proc. Natl. Acad. Sci. U.S.A. 90*, 3309–3313.
Puustinen, A. (1993) Ph.D. Thesis, University of Helsinki, Finland.
Puustinen, A., & Wikström, M. (1991) *Proc. Natl. Acad. Sci. U.S.A. 88*, 6122–6126.
Puustinen, A., Finel, M., Haltia, T., Gennis, R. B., & Wikström, M. (1991) *Biochemistry 30*, 3936–3942.
Puustinen, A., Morgan, J. E., Verkhovsky, M., Thomas, J. W., Gennis, R. B., & Wikström, M. (1992) *Biochemistry 31*, 10363–10369.
Saraste, M. (1990) *Q. Rev. Biophys. 23*, 331–366.
Schägger, H., & von Jagow, G. (1987) *Anal. Biochem. 166*, 368–379.
Shapleigh, J. P., Hill, J. J., Alben, J. O., & Gennis, R. B. (1992) *J. Bacteriol. 174*, 2338–2343.
Thomas, P. E., Ryan, D., & Wayne (1976) *Anal. Biochem. 75*, 168–176.
Weinstein, J. D., & Beale, S. I. (1983) *J. Biol. Chem. 258*, 6799–6807.
Wikström, M., Krab, K., & Saraste, M. (1981) *Cytochrome oxidase—a synthesis*, Academic Press, London.
Wood, P. M. (1984) *Biochim. Biophys. Acta 768*, 293–317.
Wu, W., Chang, C. K., Varotsis, C., Babcock, G. T., Puustinen, A., & Wikström, M. (1992) *J. Am. Chem. Soc. 114*, 1182–1187.
Yu, C.-A., Yu, L., & King, T. E. (1975) *J. Biol. Chem. 250*, 1383–1392.
Zannoni, D., & Marrs, B. L. (1981) *Biochim. Biophys. Acta 637*, 96–106.
Zannoni, D., & Daldal, F. (1993) *Arch. Microbiol. 160*, 413–423.
Zannoni, D., Baccarini-Melandri, A., Melandri, B. A., Evans, E. H., Prince, R. C., & Crofts, A. R. (1974) *FEBS Lett. 48*, 152–155.
Zannoni, D., Melandri, B. A., & Baccarini-Melandri, A. (1976) *Biochim. Biophys. Acta 423*, 413–430.
Zannoni, D., Venturoli, G., & Daldal, F. (1992) *Arch. Microbiol. 157*, 367–374.